PHYSICAL REVIEW FLUIDS **8**, 110510 (2023)

Gallery of Fluid Motion

Axisymmetric and azimuthal waves on a vibrated sessile drop

D. Panda,[1] L. Kahouadji,[1,*] L. S. Tuckerman,[2] S. Shin,[3]
J. Chergui,[4] D. Juric,[4,5] and O. K. Matar[1]

[1]*Department of Chemical Engineering, Imperial College London, London SW7 2AZ, United Kingdom*
[2]*Physique et Mécanique des Milieux Hétérogènes, CNRS, ESPCI Paris, Université PSL, Sorbonne Université, Université de Paris, 75005 Paris, France*
[3]*Department of Mechanical and System Design Engineering, Hongik University, Seoul 04066, Republic of Korea*
[4]*Université Paris Saclay, Centre National de la Recherche Scientifique (CNRS), Laboratoire Interdisciplinaire des Sciences du Numérique (LISN), 91400 Orsay, France*
[5]*Department of Applied Mathematics and Theoretical Physics, University of Cambridge, Cambridge CB3 0WA, United Kingdom*

(Received 15 July 2023; published 16 November 2023)

This paper is associated with a poster winner of a 2022 American Physical Society's Division of Fluid Dynamics (DFD) Gallery of Fluid Motion Award for work presented at the DFD Gallery of Fluid Motion. The original poster is available online at the Gallery of Fluid Motion, https://doi.org/10.1103/APS.DFD.2022.GFM.P0027

DOI: 10.1103/PhysRevFluids.8.110510

There is a growing interest in understanding the dynamics of vibrated sessile drops due to technological innovations in adaptive liquid lenses [1] and drop atomization in heat transfer cells [2]. Noblin *et al.* [3] observed that at low forcing amplitudes, the drops exhibited axisymmetric standing waves with pinned contact lines on polystyrene surfaces. At higher amplitudes, the drops exhibited azimuthal (nonaxisymmetric) modes punctuated by stick-slip contact line motion. Vukasinovic *et al.* [4] found that vibration-induced drop atomization follows the appearance of the azimuthal waves along the contact line beyond a threshold acceleration. They also observed that the contact line was pinned, irrespective of the acceleration amplitude. The axisymmetric and azimuthal waves exhibit harmonic and subharmonic responses, respectively.

We performed 3D numerical simulations of a hemi-ellipsoidal drop of volume $\mathcal{V} = 100\,\mu L$, contact radius $R_c = 4.12$ mm, and height $h = 3\mathcal{V}/(2\pi R_c^2)$ as in [4]. We use an in-house multiphase solver, *BLUE* [5] previously used to study spherical Faraday waves [6]. The computational domain, a half cube of dimensions 12 mm × 12 mm × 6 mm, encompassing water and air, is decomposed into 12×12×6 cores each of resolution 64^3, leading to a global mesh structure of 768×768×384 grid cells of size $\Delta x = 15.625$ μm. With approximately 56 grid points per axisymmetric and azimuthal wave length, the waves are sufficiently resolved.

The density of water and air are set to 998 kg/m^3 and 1.205 kg/m^3, and their dynamic viscosities to 10^{-3} kg/ms and 1.82×10^{-5} kg/ms, respectively. The surface tension is equal to 0.0714 N/m.

*l.kahouadji@imperial.ac.uk

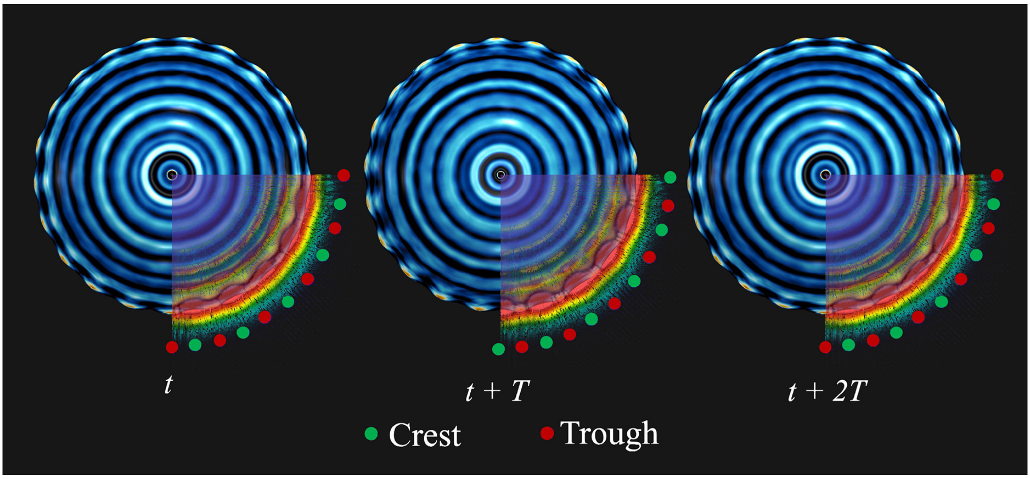

FIG. 1. Top view of drop (100 μL) oscillations with $f = 1040\,\mathrm{Hz}$ and $a = 1000\,\mathrm{m/s^2}$ at t, $t + T$, and $t + 2T$, respectively. Here $t = 32T + T/2$ and $T = 1/f$.

The substrate is vibrated at a frequency $f = 1040$ Hz. As an initial condition, we used a perturbation proportional to the 10th axisymmetric spherical harmonic $Y_{10}^{(0)}$ to resemble the axisymmetric waves. We ramped up the acceleration to $a = 1000$ m/s^2 at a rate of 100 m/s^2 every 20 forcing time periods. Although the final acceleration is substantially higher than the threshold acceleration for the azimuthal waves obtained in the experiments, this procedure reduces the computational expense since the azimuthal variation appears more quickly.

We imposed periodic and Neumann boundary conditions on the velocity at the lateral and top faces of the water-air cubical domain, respectively. Near-contact line azimuthal waves were observed only when a generalized Navier (rather than a Dirichlet) boundary condition was imposed on the substrate, with hysteresis characterized by advancing and receding contact angles of $\theta_a = 90^\circ$ and $\theta_r = 84^\circ$, respectively. This contradicts the experiments of [4], in which the contact line remained pinned.

Figure 1 shows that the near-contact line wave crests (green) and troughs (red) occur at the same locations at $t + 2T$, but not at $t + T$, demonstrating that these are subharmonic standing waves. Conversely, the axisymmetric waves repeat after each time period T, exhibiting a harmonic response. These observations agree well with the experiments [4]. Although a subharmonic response is a classic signature of Faraday waves [7], such waves oscillate in the same direction as the imposed oscillation. Thus, if the radially oscillating azimuthal waves near the contact line result from a Faraday-type instability, the instability is not engendered by the vertically oscillating substrate, but by the radially oscillating axisymmetric waves, as proposed in [4]. However, the azimuthal waves might be caused instead by a modulation of the axisymmetric waves brought about by the proximity of the substrate to the contact line.

The subharmonic azimuthal waves grow on the interface, superposed on the harmonic axisymmetric waves, as shown in Fig. 2. Like quasipatterns in two-frequency gravity modulation caused by mixing two unstable wave vectors [8], the harmonic and subharmonic wave vectors form an n-fold symmetric lattice which eventually breaks down to become chaotic, as found in the experiments. The chaotic mixing leads to the formation of negative curvature craters, which eventually form jets that undergo end-pinching leading to droplet atomization.

Our observations await a more detailed understanding of the physics of vibrating sessile drops. Although the harmonic axisymmetric waves may be the cause of the subharmonic azimuthal waves, a number of crucial questions need to be addressed. Among these are (i) the role of the contact line in the formation of subharmonic azimuthal waves; (ii) the role of the vibrating substrate in the

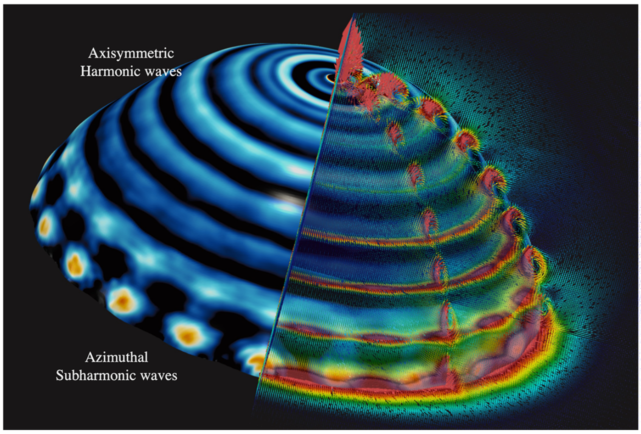

FIG. 2. Snapshot of vibrated drop at $t = 32T + T/2$. The velocity glyphs illustrate the vortices on the axisymmetric waves and the strong influx at the contact line. Pressure contours on the interface show high pressure zones at the crests on the drop apex and in the vicinity of the contact line. The parameter values remain unaltered from Fig. 1.

growth of these waves on the interface; and (iii) an understanding of such subharmonic waves when the external vibrations are parallel to the interface, e.g., oscillatory Kelvin-Helmholtz instability [9]. Addressing these issues will be the subject of future work.

This work was supported by the Engineering and Physical Sciences Research Council, UK, through the MEMPHIS (EP/K003976/1) and PREMIERE (EP/T000414/1) programme grant. O.K.M. acknowledges funding from PETRONAS and the Royal Academy of Engineering for a Research Chair in Multiphase Fluid Dynamics. D.P. acknowledges the Imperial President's PhD scholarship. D.P. and L.K. acknowledge HPC facilities provided by the Imperial College London Research Computing Service. D.J. and J.C. acknowledge support through HPC/AI computing time at the Institut du Developpement et des Ressources en Informatique Scientifique (IDRIS) of the Centre National de la Recherche Scientifique (CNRS), coordinated by GENCI (Grand Equipement National de Calcul Intensif) Grant No. 2023 A0142B06721. The numerical simulations were performed with code BLUE [5] and the visualizations were generated using ParaView.

[1] C. A. López, C.-C. Lee, and A. H. Hirsa, Electrochemically activated adaptive liquid lens, Appl. Phys. Lett. **87**, 134102 (2005).

[2] S. N. Heffington, and W. Z. Black, and A. Glezer, Vibration-induced droplet atomization heat transfer cell for high-heat flux applications, in *Proceedings of the Eighth Intersociety Conference on Thermal and Thermomechanical Phenomena in Electronic Systems, San Diego, CA* (IEEE, New York, 2002), pp. 408–412.

[3] X. Noblin, A. Buguin, and F. Brochard-Wyart, Vibrations of sessile drops, Eur. Phys. J. Spec. Top. **166**, 7 (2009).

[4] B. Vukasinovic, M. K. Smith, and A. Glezer, Dynamics of a sessile drop in forced vibration, J. Fluid Mech. **587**, 395 (2007).

[5] S. Shin, J. Chergui, and D. Juric, A solver for massively parallel direct numerical simulation of three-dimensional multiphase flows, J. Mech. Sci. Technol. **31**, 1739 (2017).

[6] A.-H. Ebo-Adou, L. S. Tuckerman, S. Shin, J. Chergui, and D. Juric, Faraday instability on a sphere: Numerical simulation, J. Fluid Mech. **870**, 433 (2019).

[7] M. Faraday, On a peculiar class of acoustical figures; and on certain forms assumed by groups of particles upon vibrating elastic surfaces, Philos. Trans. R. Soc. **121**, 299 (1831).

[8] W. S. Edwards and S. Fauve, Patterns and quasi-patterns in the Faraday experiment J. Fluid Mech. **278**, 123 (1994).

[9] H. N. Yoshikawa and J. E. Wesfreid, Oscillatory Kelvin–Helmholtz instability. Part 1. A viscous theory, J. Fluid Mech. **675**, 223 (2011).